Role of the Maritime Continent in the remote influence of Atlantic Niño on the Pacific

Siying Liu[1], Ping Chang[2*], Xiuquan Wan[1,3*], Stephen G. Yeager[4], Ingo Richter[5]

[1]College of Oceanic and Atmospheric Sciences, Ocean University of China, 238 Songling Rd, Qingdao, 266100, Shandong, China.

[2*]Department of Oceanography, Texas A&M University, 400 Bizzell St, College Station, 77843, Texas, USA.

[3*]Physical Oceanography Laboratory/CIMST, Ocean University of China and Qingdao National Laboratory for Marine Science and Technology, 168 Wenhai Middle Rd, Qingdao, 266100, Shandong, China.

[4]National Center for Atmospheric Research, Boulder, Colorado, USA.

[5]Application Laboratory (APL), Research Institute for Value - Added - Information Generation (VAiG), Japan Agency for Marine - Earth Science and Technology (JAMSTEC), Yokohama, Japan

*Corresponding authors. E-mails: ping@tamu.edu; xqwan@ouc.edu.cn;

Contributing authors: liusiying@stu.ouc.edu.cn; yeager@ucar.edu; richter@jamstec.go.jp;

Supplementary Figures

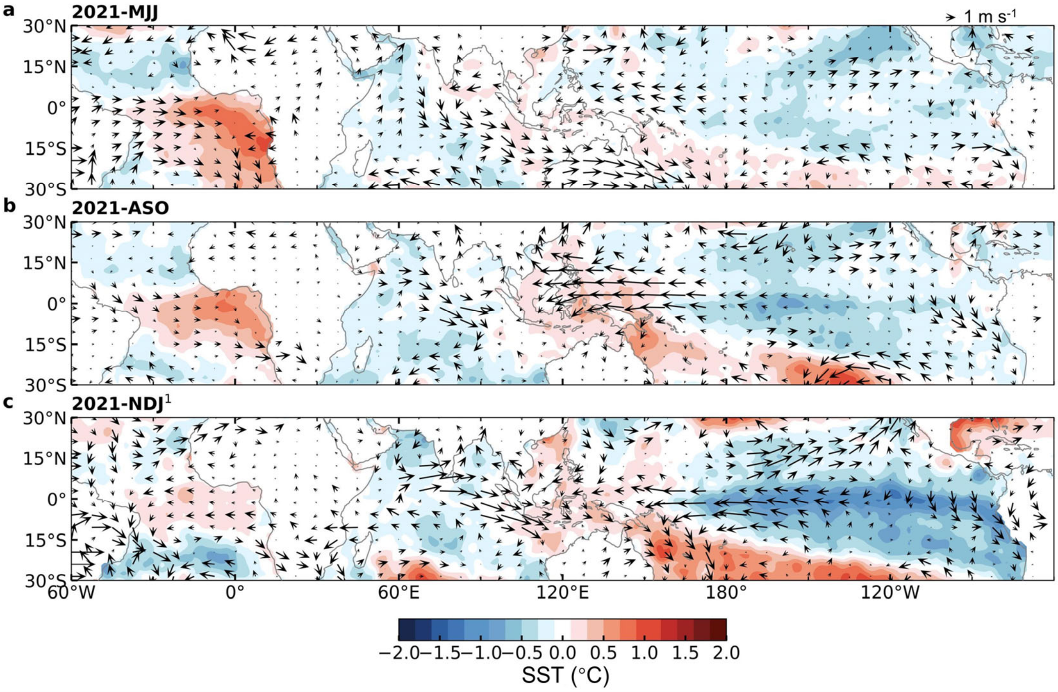

Supplementary Figure. S1 | The Atlantic Niño and Pacific La Niña events during 2021-2022 in reanalysis and observation. a-c, detrended SST (°C; color shading) anomalies and wind anomalies at 850 hPa (m s^{-1}; arrows) over the boreal summer (May-June-July (MJJ)) (**a**), fall (August-September-October (ASO)) (**b**) and winter (November-December-January (NDJ^1)) (**c**) in 2021-2022 from HadISST and ERA5 Reanalysis respectively.

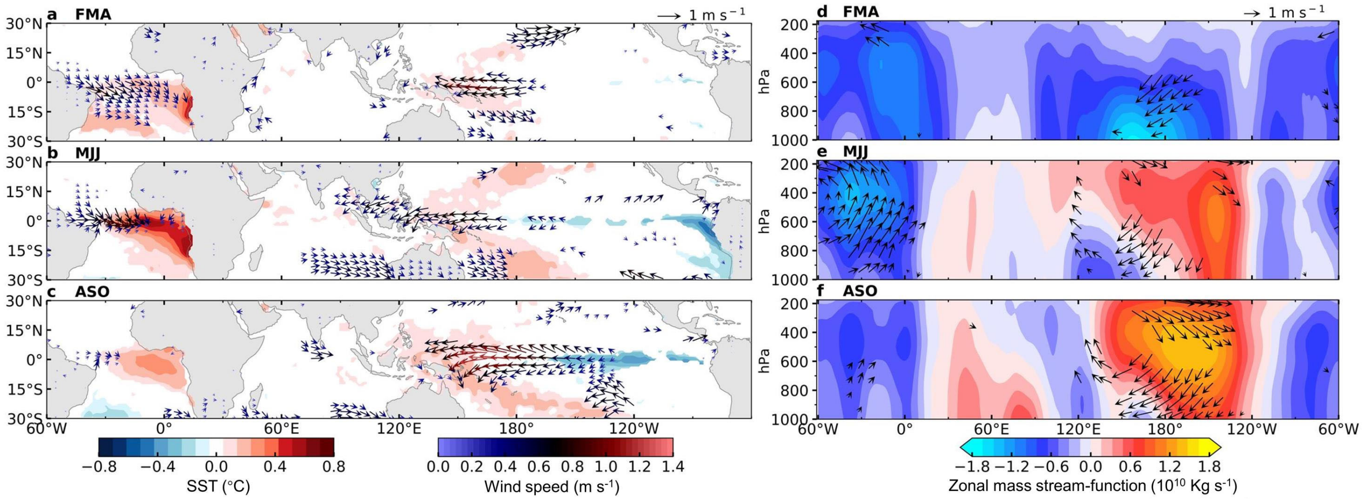

Supplementary Figure. S2 | Observed tropical SST and Walker Circulation anomalies response to Atlantic Niño excluding the strong ENSO years. a-c, Boreal spring (February-March-April (FMA)) (**a**), summer (May-June-July (MJJ)) (**b**), and fall (August-September-October (ASO)) (**c**) SST (°C; color shading) anomalies (HadISST, 1959-2021) and wind anomalies at 1000hPa (m s^{-1}; color arrows) averaged by three reanalysis datasets (ERA5, JRA55 for 1959-2021 and ERA-Interim for 1979-2018) regressed onto the normalized May-June-July (MJJ) ATL3 index after first excluding the years of strong ENSO from the data record (Methods). **d-f**, same as **a-c** except for zonal and vertical wind anomalies (m s^{-1}; arrows; vertical winds multiplied by 100.) averaged from 5°S to 5°N and zonal mass stream-function anomalies (Kg s^{-1}; color shading; see Methods) at 175-1000 hPa pressure levels. The colors and vectors indicate statistically significant at 10% level based on a two-sided Student's t-test. The statistical test was not performed for the zonal mass stream-function because its main purpose is to illustrate the direction of the zonal circulations.

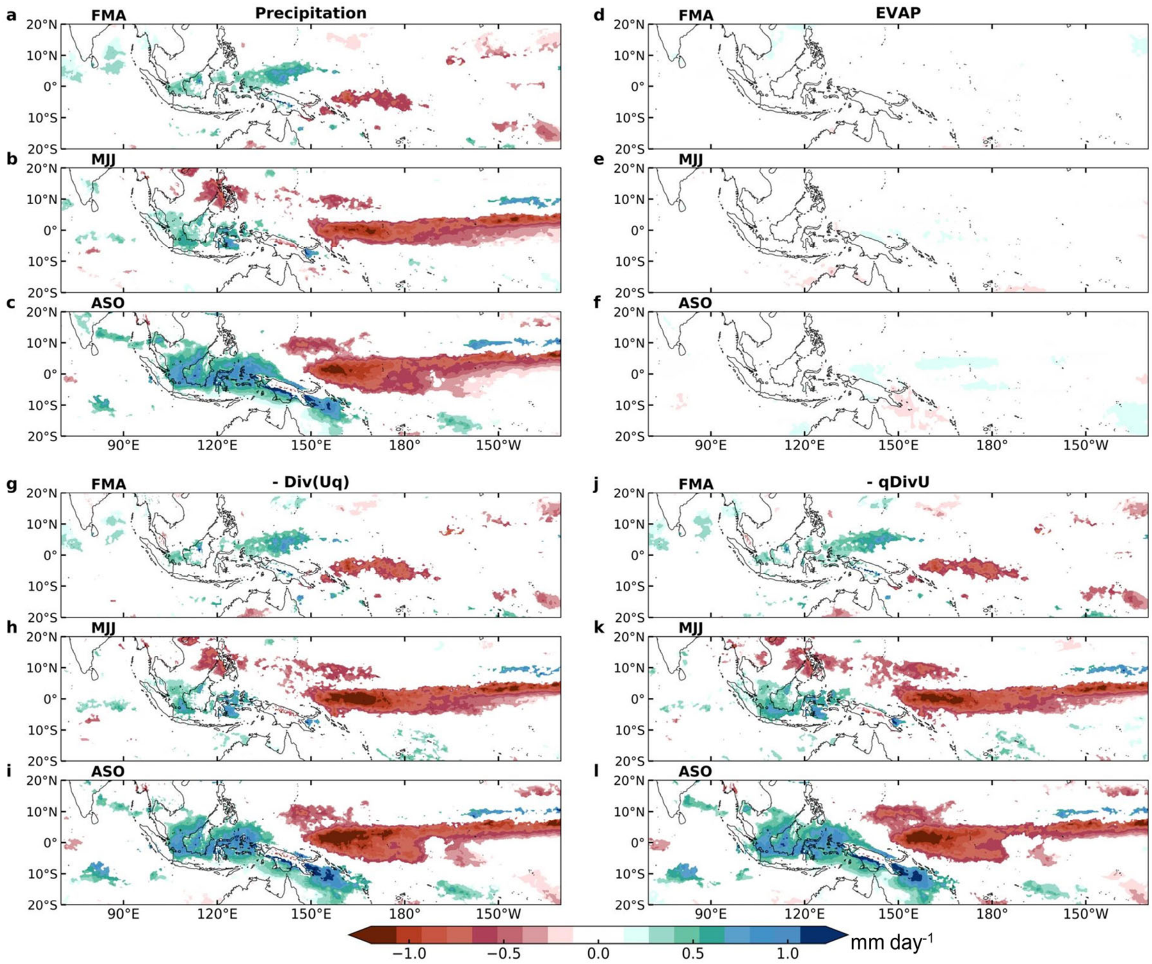

Supplementary Figure. S3 | Response of precipitation and moisture-related terms in the MC-WP region to Atlantic Niño in reanalysis on seasonal timescales. a-c, Boreal spring (February-March-April (FMA)) (**a**), summer (May-June-July (MJJ)) (**b**), and fall (August-September-October (ASO)) (**c**) precipitation (mm day^{-1}; color shading) anomalies in reanalysis datasets (ERA5, 1959-2021) regression against the normalized May-June-July (MJJ) ATL3 index after linearly regressing out ENSO-related variability from the data record (Methods). **d-f**, same as **a-c** except for evaporation (mm day^{-1}; color shading). **g-i**, same as **a-c** except for vertical integral of divergence of moisture flux multiplied by -1 (mm day^{-1}; color shading; referred as -Div(Uq)). **j-l**, same as **a-c** except for vertically integrated moisture divergence multiplied by -1 (mm day^{-1}; color shading; referred as -qDivU).

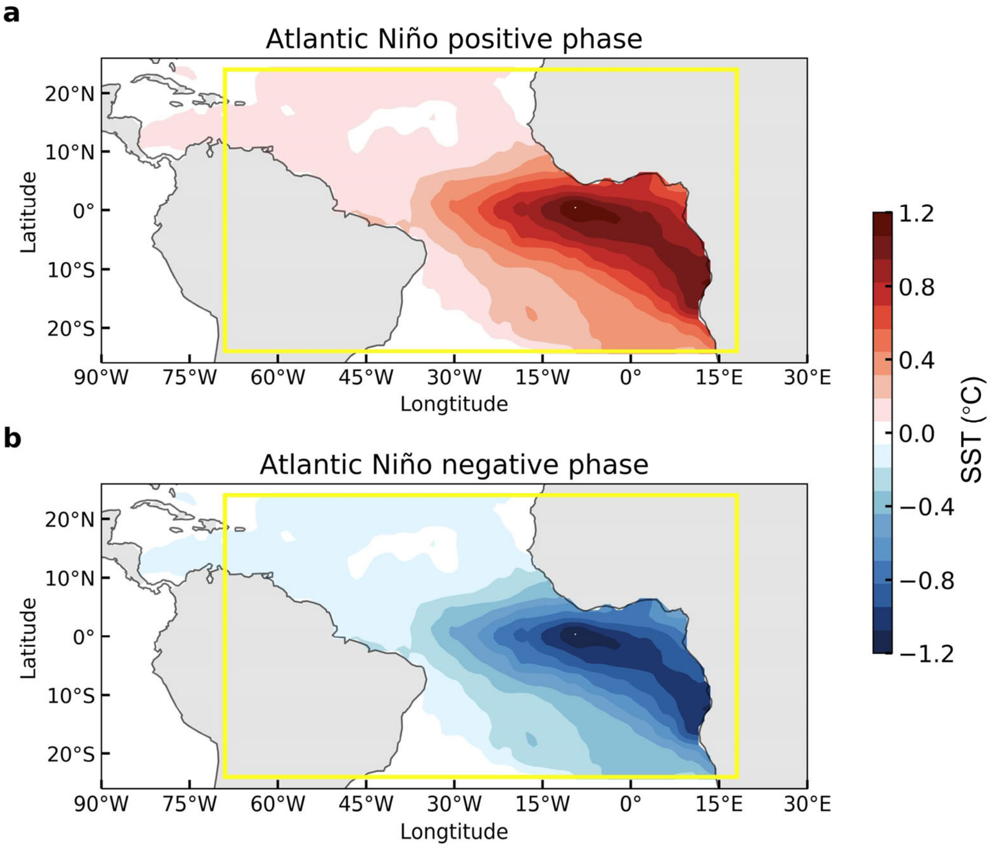

Supplementary Figure. S4 | Atlantic Niño SST anomalies spatial pattern derived from observation for the three large ensembles. a-b, SST anomalies (°C; color shading) from HadISST datasets during 1870-2017 regressed onto the June-July-August (JJA) ATL3 index multiplied by +1 for CTRL+, NTOP+ and NFRC+ simulations (**a**) and by -1 for CTRL-, NTOP- and NFRC- simulations (**b**) respectively. The yellow boxes in (**a-b**) show regions performing SST restoring skill in simulation.

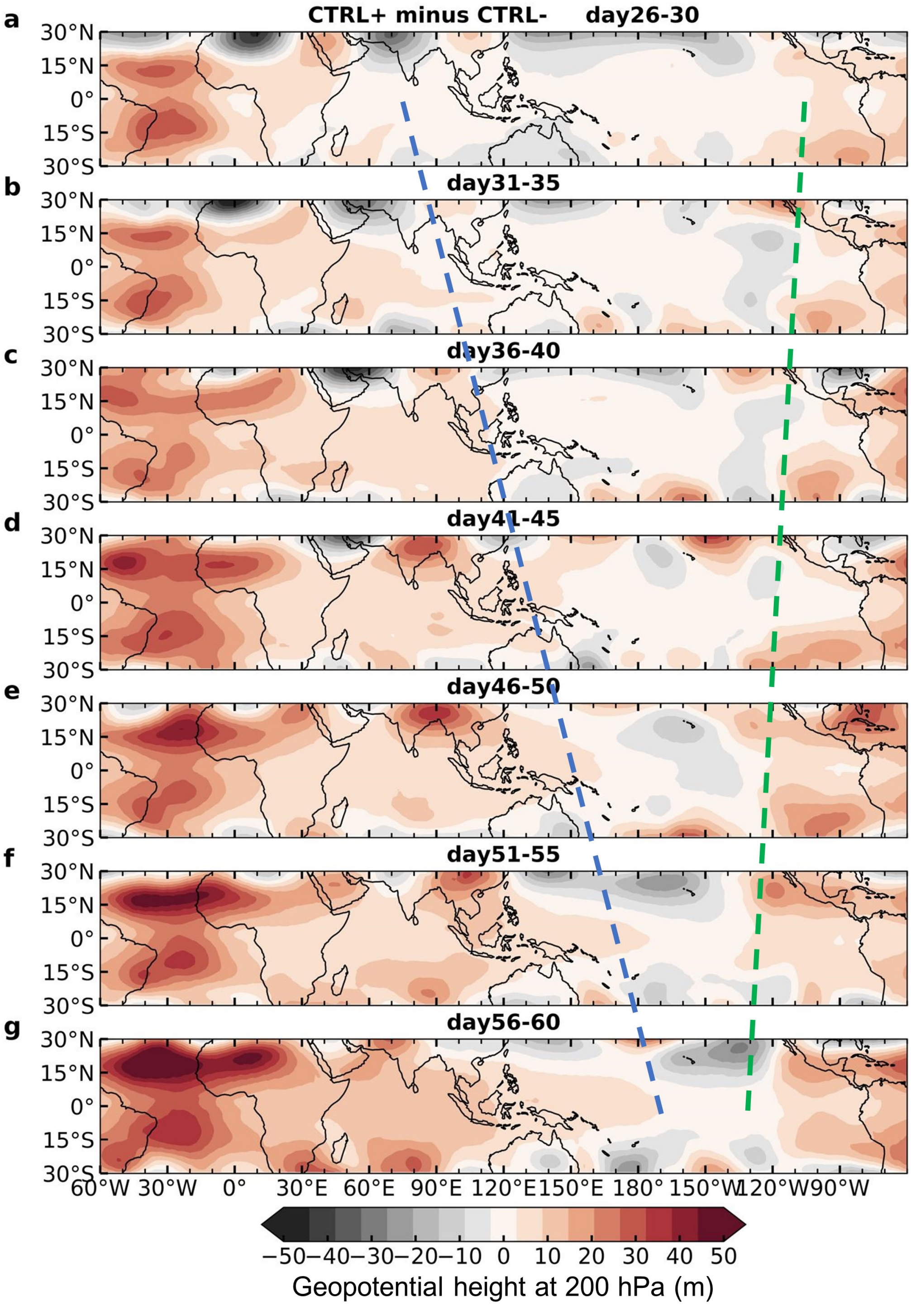

Supplementary Figure. S5 | Eastward propagating atmospheric Kelvin waves and westward propagating Rossby waves in the CTRL ensemble. a-g, simulated 5-day mean geopotential height anomalies at 200 hPa (m; color shading) during 26-30 (**a**), 31-35 (**b**), 36-40 (**c**), 41-45 (**d**), 46-50 (**e**), 51-55 (**f**), and 56-60 (**g**) days in the CTRL ensemble. Anomalies are obtained by ensemble-mean of CTRL+ minus CTRL-. Eastward propagation of atmosphere Kelvin wave and westward propagation of Rossby wave are indicated by blue and green dashed lines respectively.

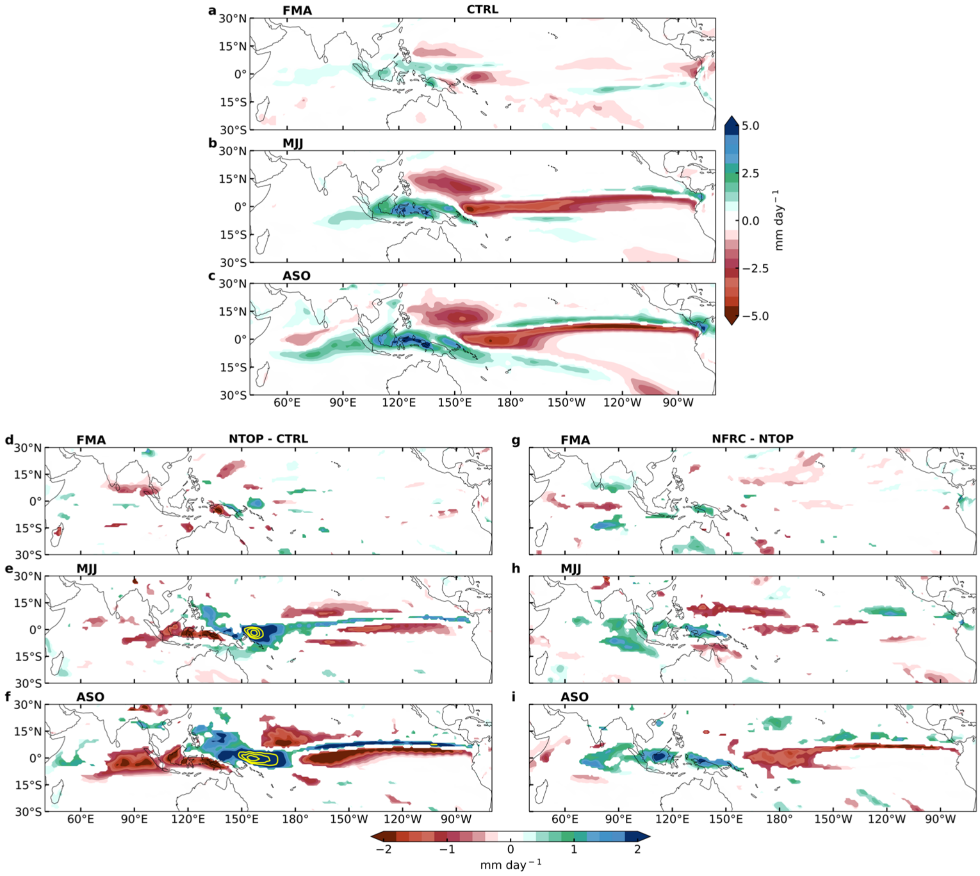

Supplementary Figure. S6 | Simulated response of precipitation to Atlantic Niño SST in the three sets of large ensemble experiments. a-c, Simulated precipitation (mm day^{-1}; color shading) averaged over boreal spring (FMA) (**a**), summer (MJJ) (**b**) and fall (ASO) (**c**) for CTRL; **d-f**, same as **a-c** except for the anomalies in NTOP minus those in CTRL. The heavy differences of precipitation in (**d-f**) are indicated by the yellow contour lines at 3, 4, 5 mm day^{-1}. **g-i**, same as **a-c** except for the anomalies in NFRC minus those in NTOP. Anomalies in CTRL, NTOP and NFRC are obtained by CTRL+ minus CTRL-, NTOP+ minus NTOP-, and NFRC+ minus NFRC-, respectively. Colors represent those that are significant at the 10% level based on a two-sided Student's t-test. Note that in **d-f** and **g-i** the tropical Atlantic sector is excluded because the forcing is the same for all three ensembles.

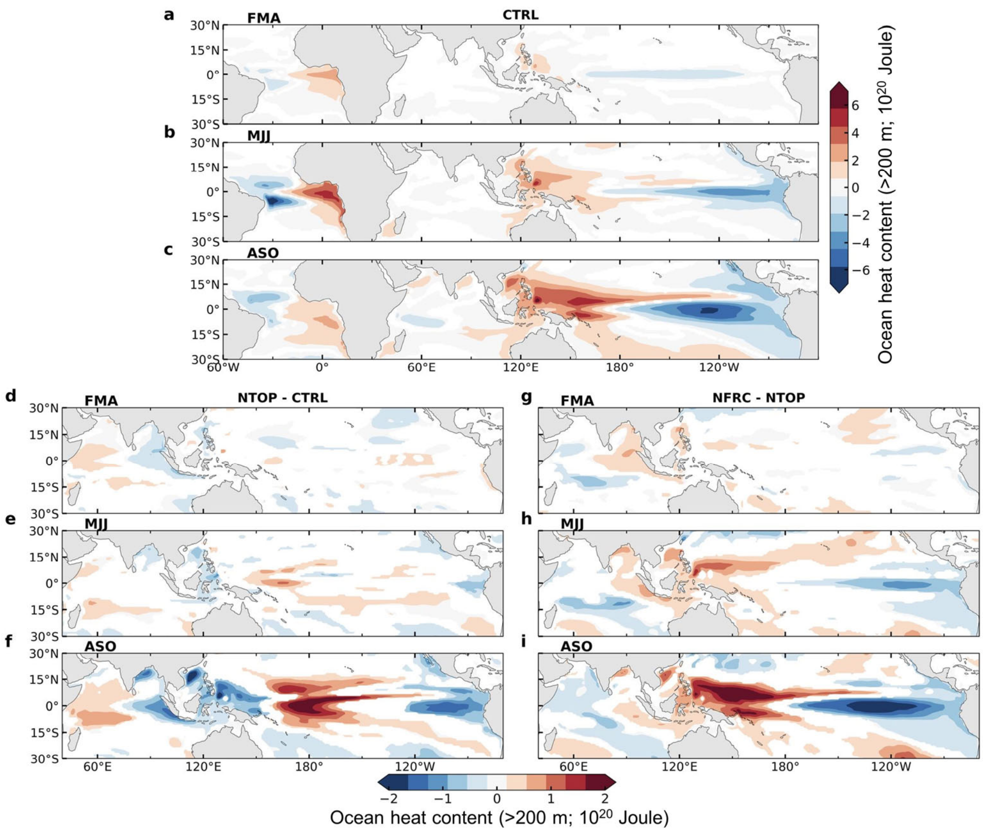

Supplementary Figure. S7 | Simulated response of ocean heat content to Atlantic Niño SST in the three sets of large ensemble experiments. a-c, simulated ocean heat content (10^{20} Joule; color shading) in upper 200 meters averaged over the boreal spring (FMA) (**a**), summer (MJJ) (**b**) and fall (ASO) (**c**) for CTRL; **d-f**, same as **a-c** except for the anomalies in NTOP minus those in CTRL. **g-i**, same as **a-c** except for the anomalies in NFRC minus those in NTOP. Anomalies in CTRL, NTOP and NFRC are obtained by CTRL+ minus CTRL-, NTOP+ minus NTOP-, and NFRC+ minus NFRC-, respectively. Colors represent those that are significant at the 10% level based on a two-sided Student's t-test. Note that in **d-f** and **g-i** the tropical Atlantic sector is excluded because the forcing is the same for all three ensembles.

a

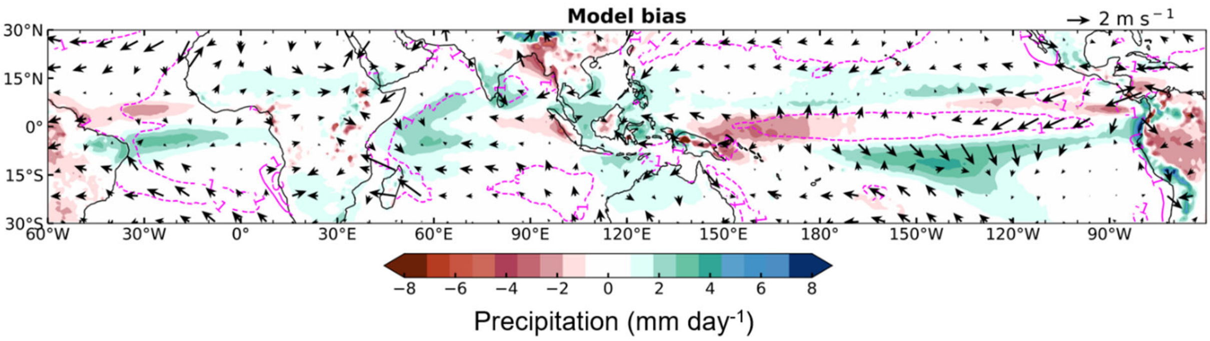

Supplementary Figure. S8 | CESM1 model biases in the tropics. Simulated SST (°C; contours), wind at 1000 hPa (m s^{-1}; arrows) and precipitation (mm day^{-1}; color shading) biases reference to HadISST datasets and ERA5 Reanalysis for 1959-2021. The model means are derived from a 2200-year preindustrial CESM1 simulation at nominal ~1°resolution for the period of year 1500 to year 1562 - the same 63-year period as in observations.

Supplementary Tables

Supplementary Table 1 Observation and reanalysis for lag-regression.

Datasets	Variables	Periods	Temporal resolution	Horizontal resolution	Vertical levels
HadISST	SST	1959-2021	monthly	1° x 1°	none
ERA5 Reanalysis	horizontal and vertical wind vectors	1959-2021		0.25° x 0.25°	1000, 975, 950, 925, 900, 875, 850, 800, 750, 700, 650, 600, 550, 500, 450, 400, 350, 300, 250, 200, and 175 hPa
ERA-Interim Reanalysis		1979-2018		0.703° x ~0.702°	
JRA55 Reanalysis		1959-2021		1.25° x 1.25°	

Supplementary Table 2 Years (January-December) used for lag-regression.

No pre-existing ENSO years for lag-regression (44 years)
1960, 1961, 1962, 1963, 1964, 1965, 1967, 1968, 1969, 1970, 1972, 1975, 1977, 1978, 1979, 1980, 1981, 1982, 1984, 1986, 1988, 1990, 1991, 1993, 1994, 1995, 1996, 1997, 2001, 2002, 2003, 2004, 2005, 2006, 2007, 2009, 2012, 2013, 2014, 2015, 2017, 2018, 2019, 2020